Quasiclassical trajectory study of the $SiH_4+H \rightarrow SiH_3+H_2$ reaction on a global *ab initio* potential energy surface

Manhui Wang,[1,2,a)] Xiaomin Sun,[3] and Wensheng Bian[1,b)]
[1]*Beijing National Laboratory for Molecular Sciences, State Key Laboratory of Molecular Reaction Dynamics, Institute of Chemistry, Chinese Academy of Sciences, Beijing 100190, People's Republic of China*
[2]*Graduate School of Chinese Academy of Sciences, Beijing 100190, People's Republic of China*
[3]*Institute of Chemistry, Chinese Academy of Sciences, Beijing 100190, People's Republic of China and Environment Research Institute, Shandong University, Jinan 250100, People's Republic of China*

(Received 19 February 2008; accepted 28 July 2008; published online 28 August 2008)

The $SiH_4+H \rightarrow SiH_3+H_2$ reaction has been investigated by the quasiclassical trajectory (QCT) method on a recent global *ab initio* potential energy surface [M. Wang *et al.*, J. Chem. Phys. **124**, 234311 (2006)]. The integral cross section as a function of collision energy and thermal rate coefficient for the temperature range of 300–1600 K have been obtained. At the collision energy of 9.41 kcal/mol, product energy distributions and rovibrational populations are explored in detail, and H_2 rotational state distributions show a clear evidence of two reaction mechanisms. One is the conventional rebound mechanism and the other is the stripping mechanism similar to what has recently been found in the reaction of CD_4+H [J. P. Camden *et al.*, J. Am. Chem. Soc. **127**, 11898 (2005)]. The computed rate coefficients with the zero-point energy correction are in good agreement with the available experimental data. © *2008 American Institute of Physics*.
[DOI: 10.1063/1.2973626]

I. INTRODUCTION

The $SiH_4+H \rightarrow SiH_3+H_2$ reaction plays a significant role in the chemical vapor deposition (CVD) processes used in the semiconductor industry.[1–4] As a prototype of exothermic polyatomic hydrogen abstraction reactions, its kinetics has been extensively studied experimentally in the past decades. The rate coefficients have been measured with a wide variety of experimental methods,[5–16] but most work has been carried out at room temperature and only a few recent studies[10,11,16] reported the temperature dependence of the rate coefficient. For example, Arthur and Miles[11] presented the rate coefficient in the form, $k=(7.49\pm0.49)\times10^{-11}\exp[(-1610\pm25)/T]$ cm^3 molecule^{-1} s^{-1} for the temperature range of 298–636 K in 1997; Goumri *et al.*[16] gave the rate coefficient in the temperature range of 290–660 K to be $k=(1.78\pm0.11)\times10^{-10}\exp[-(16.0\pm0.2)\ \text{kJ mol}^{-1}/RT]$ cm^3 molecule^{-1} s^{-1} in 1993. Various experimental rate coefficients at room temperatures have varied from 85.0×10^{-13} to 2.0×10^{-13} cm^3 molecule^{-1} s^{-1}, and the variation range has recently been reduced to 4.0×10^{-13}–2.0×10^{-13} cm^3 molecule^{-1} s^{-1}.[10–16] However, a detailed state-resolved dynamical experimental investigation is still lacking for the title reaction.

On the other hand, there have been some theoretical studies on the title reaction. Early *ab initio* calculations[17,18] were focused on the stationary points along the minimum energy path (MEP). Gordon *et al.*[17] and Tachibana *et al.*[18] optimized the geometries of the stationary points at the Hartree–Fock level and then performed single-point calculations to include electron-correlation effects using a variety of *ab initio* methods with the basis set of 6-31G** or smaller. Later, a theoretical rate coefficient was reported by several groups based on *ab initio* calculations. Goumri *et al.*,[16] and Dobbs and Dixon[19] performed *ab initio* calculations with the geometries optimized at the second order Møller–Plesset (MP2) level and then investigated the rate coefficient using conventional transition state theory (TST) with a simple Wigner tunneling factor. In 1998, Espinosa-García *et al.*[20] reported a semiempirical potential energy surface (PES) for the title reaction, which utilized an analytical functional form based on London–Eyring–Polanyi (LEP) expressions with parameters to reproduce the reactant and product experimental properties and the *ab initio* saddle point properties. Using this surface, Espinosa-García[20] evaluated rate coefficients with variational TST (VTST). In 2000, Yu *et al.*[21] carried out the direct dynamics studies using VTST based on their *ab initio* calculations on MEP. Recently, VTST calculations[22] were performed on a global *ab initio* PES (see below for more details), yielding rate coefficients in good general agreement with the available experimental data, and some preliminary classical trajectory calculations were also carried out on this PES. Most recently, Wang *et al.*[23] reported rate coefficients and kinetic isotope effects on the semiempirical PES of Espinosa-García *et al.*[20] using the quantum instanton approximation, which can be viewed as a quantum analog of TST. However, most of theoretical methods used in the above studies are TST and its variants, and a detailed dynamical study is still unavailable.

A global *ab initio* 12-dimensional PES for the title reaction has recently been reported by our group,[22] as is referred to as the WSB surface. The details of the WSB surface have

a)Present address: School of Chemistry, Cardiff University, Main Building, Park Place, Cardiff CF10 3AT, UK.
b)Author to whom correspondence should be addressed. Electronic mail: bian@iccas.ac.cn.

been given elsewhere[22] and here we just describe the main features. The *ab initio* calculations for the energy and derivatives are based on the unrestricted quadratic configuration interaction treatment with all single and double excitations (UQCISD) together with Dunning's correlation consistent, polarized valence, triple zeta (cc-pVTZ) basis set. The modified Shepard interpolation method of Collins and co-workers[24] is applied, with which the PES is expressed as an interpolation of around 1300 *ab initio* reference points. The classical trajectory calculations at the collision energy of 9.41 kcal/mol demonstrate the convergence of the PES with respect to the size of the reference data set. The geometrical parameters and vibrational frequencies of the reactant and products and reaction enthalpy from the WSB surface show good agreement with the experimental data. The contour plots made by setting various cuts into the potential energy hypersurface are found to be reasonable in various regions. The classical potential barrier of the $SiH_4+H \rightarrow SiH_3+H_2$ reaction is 6.01 kcal/mol, and two very shallow van der Waals minima in the entrance and exit valleys are revealed on the WSB surface. Based on the abovementioned 12-dimensional PES, various detailed dynamical calculations could be performed. However, the exact 12-dimensional global quantum dynamics calculations are still unaffordable nowadays; alternatively, the quasiclassical trajectory (QCT) calculations[25,26] in full dimensionality are feasible. In fact, the QCT method has been widely used to study all kinds of dynamical problems for reaction systems involving three and four atoms[27–43] over the decades and is becoming popular in studying the reaction dynamics of larger systems.[44–49]

In the present work, we performed detailed QCT calculations on the 12-dimensional *ab initio* WSB surface[22] for the $SiH_4+H \rightarrow SiH_3+H_2$ reaction. Various dynamical quantities are obtained and reaction mechanisms are analyzed. This article is organized as follows. Section II describes the methodology and computational details for the QCT study. The results of QCT calculations are presented and discussed in Sec. III. Finally, a summary is given in Sec. IV.

II. THEORETICAL METHODS AND COMPUTATIONAL DETAILS

A detailed description of the QCT method can be found in literature.[25,26,50–55] Here, we only give some details related to the present study. All the present QCT calculations were performed using a modified version of VENUS96 (Ref. 56) customized to incorporate the WSB PES with the first derivatives.[22] Test QCT calculations with the initial conditions similar to those of the previous classical trajectory calculations[22] validated various procedures for the incorporation of programs.

For all trajectories, the Cartesian coordinates and velocities for SiH_4 were randomly oriented by rotation through Euler's angles within the SiH_4 space-fixed center-of-mass coordinate frame.[57] An integration time step of 0.05 fs was employed, which gave a conservation of the total energy better than 1 in 10^4. The trajectories were initiated at the $H+SiH_4$ asymptote with a separation of 7.94 Å (15.0 bohrs) between the two species and were terminated when the fragments, moving apart, reached the same separation. This separation is large enough so that the interaction between fragments is negligible.

For the H_2 product, the rotational quantum number j' is obtained by equating the classical rotational angular momentum to $[j'(j'+1)]^{1/2}\hbar$. The vibrational quantum number v' is obtained by Einstein-Brillouin-Keller[58] semiclassical quantization of the action integral. The noninteger j' and v' values have been rounded off to the nearest integers.

For the other product SiH_3, the instantaneous rotational energy has been evaluated as $E_r=\frac{1}{2}\vec{\omega}\cdot\vec{j}$ and the vibrational energy is calculated by $E_v=E_{\text{int}}-E_r$, where E_{int} is the total internal energy of the product.

The reaction cross section σ_R is evaluated by applying an extended closed trapezoidal approximation[59] to the usual integral form,

$$\sigma_R = 2\pi \int_0^{b_{\max}} P(b) b db \approx \pi \sum_{b_i=0}^{b_{\max}} [P(b_i)b_i + P(b_{i+1})b_{i+1}](b_{i+1}-b_i), \quad (1)$$

where $b_{\max}$ is the maximum impact parameter b and $P(b)$ is the opacity function (or reaction probability), i.e., the fraction of reactive trajectories at each impact parameter. $b_{\max}$ can be determined by calculating trajectories at fixed values of b, and systematically increasing the value of b until no reactive trajectories are obtained.

When the relative translational energy E_{rel} is chosen from the Boltzmann distribution[51] at temperature T,

$$P(E_{\text{rel}}) = \frac{E_{\text{rel}}}{(k_B T)^2} \exp\left[-\frac{E_{\text{rel}}}{k_B T}\right]. \quad (2)$$

The rate coefficient versus temperature T is then obtained by integrating the cross section,

$$k(T) = \left(\frac{8k_B T}{\pi\mu}\right)^{1/2} \int_0^{\infty} \sigma(E_{\text{rel}}) P(E_{\text{rel}}) dE_{\text{rel}} = \left(\frac{8k_B T}{\pi\mu}\right)^{1/2} \pi b_{\max}^2 \frac{N_r}{N_{\text{tot}}}, \quad (3)$$

where $\sigma(E_{\text{rel}})$ is the reaction cross section at E_{rel}, μ is the reduced mass of the two reactants, N_{tot} is the total trajectory number, and N_r is the reactive trajectory number. The statistical uncertainty of reaction cross section and rate coefficient can be estimated by $\sigma_R[(N_{\text{tot}}-N_r)/(N_{\text{tot}}N_r)]^{1/2}$ and $k(T)\times[(N_{\text{tot}}-N_r)/(N_{\text{tot}}N_r)]^{1/2}$, respectively.

In this paper, we performed the following QCT calculations. Firstly, in order to obtain the cross section at given collision energy, batches of 10 000, 10 000, 8000, 5000, 5000, and 5000 trajectories were integrated at the collision energies of 0.0086, 0.01, 0.015, 0.02, 0.03, and 0.04 a.u. (i.e., 5.40, 6.28, 9.41, 12.55, 18.83, and 25.10 kcal/mol), respectively. The SiH_4 molecule in its rovibrational ground state was chosen using fixed normal mode sampling. To estimate $b_{\max}$, batches of 3000 trajectories were run at fixed impact parameter b, which was increased by interval of

0.5 or 0.1 Å from the initial value of 0.0 Å and, finally, no reactive trajectory was found when b was set around 3.4 Å for various collision energies. So, the impact parameter was chosen randomly between 0 and 3.5 Å, which ensures that all reactive trajectories can be collected. Secondly, to gain some insights into the product rovibrational populations and internal energy distributions, three batches of 25 000 trajectories at the collision energy E_t=0.015 a.u. (or 9.41 kcal/mol) were calculated for three impact parameters (b=0, 1.2, and 1.9 Å, respectively) with the initial SiH_4 molecule in its rovibrational ground state. In all above trajectories, the SiH_4 molecule has a random initial orientation. Finally, QCT calculations were also performed to obtain the thermal rate coefficient for the temperature range of 300–1600 K. At each temperature, the number of evaluated trajectories was chosen large enough to ensure a number of reactive trajectories occur. The relative translational energy was randomly selected to mimic the Boltzmann distribution for the chosen temperature, the vibrational energy of SiH_4 molecule was thermally sampled except that the fixed normal mode sampling was used at very low temperatures (300 K), and the rotational energy about each principal axis of inertia of SiH_4 was taken as $k_BT/2$. The values of b_{max} were determined empirically and by examining batches of 5000 trajectories at increasing impact parameters for various temperatures. The impact parameter was chosen randomly between 0 and 3.5 Å, which is found to be sufficient for collecting all contributions to the reaction for various temperatures.

A problem in QCT calculations is how to handle the quantum-mechanical zero-point energy (ZPE) in the classical mechanics simulation. Quantum mechanically, each internal molecular mode must contain an amount of energy at least equal to its ZPE. However, in classical trajectories, the energy can flow freely among all the modes without ZPE constraint, possibly yielding behavior which is not allowed in quantized real world (e.g., a molecule with a vibrational energy below its ZPE). To fix this problem in QCT calculations, some strategies[60–65] have been proposed but no completely satisfactory scheme has emerged. Here, in order to correct the ZPE leakage, we employed a so-called nonactive method,[65,66] which follows the genuine QCT approach but discards from statistics any nonphysical trajectory that is found to violate the specified physical criteria. First, the trajectories are included in statistical analysis if the sum of the final products (two polyatomic fragments are formed for the title reaction) satisfies the ZPE requirement. That is, the trajectories for which the vibrational energy of the two fragments (or complex prior to separation) is smaller than the sum of the ZPEs for the two products, are discarded from the statistical analysis. Besides the ZPE constraint in products, the ZPE at transition state also plays a role in some cases. Aoiz *et al.*[26] found that the QCT calculation would overestimate the reactivity due to the classical neglect of the ZPE constraint at transition state for some systems. For the reaction studied here, the ZPE of the transition state is comparable to the collision energy, and to correct the ZPE effect at the transition state, we introduce further modification, as described in Ref. 49, into the above treatment. In brief, the reactive trajectories, in which the initial total energy is lower than the sum of the classical energy of transition state and its harmonic ZPE, were also discarded. The scheme explained above is adopted to correct the computed cross sections and thermal rate coefficients for the title reaction.

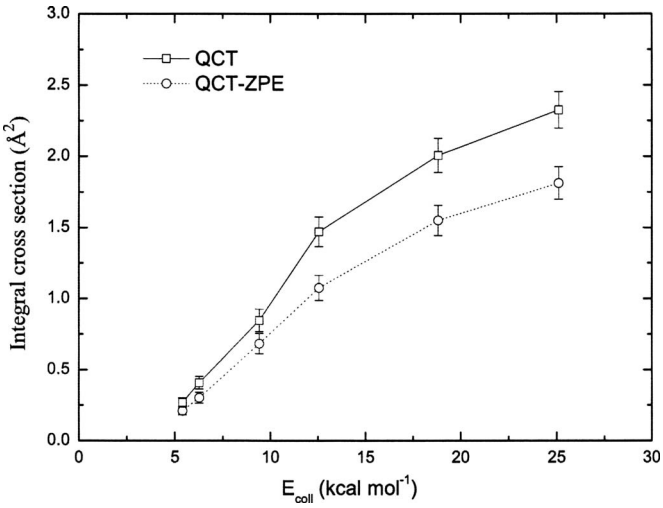

FIG. 1. Excitation function for the $SiH_4+H \rightarrow SiH_3+H_2$ reaction. The solid line with squares displays the QCT results, whereas the dotted line with circles gives the QCT-ZPE results. The initial SiH_4 molecule is in its rovibrational ground state.

III. RESULTS AND DISCUSSION

The QCT calculations, as described in the last section, are performed on the WSB surface and the excitation function, H_2 rovibrational population, product energy distribution, and thermal rate coefficient are obtained, which are presented and discussed in the following.

A. Excitation function

The excitation function, i.e., the integral cross section as a function of the collision energy, is calculated in the collision energy range from 5.40 to 25.10 kcal/mol. The values of b_{max} for various collision energies are found to be very close to one another (around 3.4 Å), which is within the internuclear distance (4.87 Å) of the van der Waals complex[22] in the entrance valley but larger than the sum (2.22 Å) of bond lengths of Si–H in SiH_4 and H–H in H_2. Results from both the QCT and ZPE-corrected QCT (QCT-ZPE) calculations are reported in Fig. 1. As can be seen, both QCT and QCT-ZPE calculations predict a reaction threshold of $\sim$5.0 kcal mol^{-1}, which is consistent with the conventional transition state enthalpy of activation at 0 K ($\Delta H_0^{\neq} \approx 5.2$ kcal mol^{-1}). The reaction cross sections increase sharply with the collision energy at low energies (the slope is around 0.12 Å^2/kcal mol for the QCT-ZPE curve), while the increase becomes less pronounced at higher energies (the slope is about 0.06 Å^2/kcal mol for the QCT-ZPE curve). Furthermore, the reaction cross sections are very sensitive to the ZPE leakage over the range of collision energy since both the classical reaction barrier height (6.01 kcal/mol) and the transition state ZPE (18.97 kcal/mol) are comparable to the

TABLE I. Relative vibrational populations of the H_2 product for the H $+SiH_4$ reaction at the collision energy of 9.41 kcal/mol for $b=0,1,2,1.9$ Å, respectively. The rovibrational ground state of SiH_4 is chosen as the initial state.

	$v'=0$	$v'=1$	$v'=2$
$b=0.0$ Å	$(82.7\pm2.1)\%$	$(16.8\pm1.0)\%$	$(0.5\pm0.1)\%$
$b=1.2$ Å	$(81.0\pm2.2)\%$	$(16.7\pm1.1)\%$	$(0.3\pm0.1)\%$
$b=1.9$ Å	$(80.2\pm2.6)\%$	$(18.9\pm1.3)\%$	$(0.9\pm0.2)\%$

collision energy. There are approximately 30% of trajectories breaking the ZPE constraint. The original QCT curve provides an upper limit for the cross section.

Much larger reaction cross sections for the title reaction were obtained than for the reaction $CH_4+H\rightarrow CH_3+H_2$ (Ref. 67) at the same collision energy. This is understandable since the title reaction has a lower barrier and a smaller threshold energy than $CH_4+H\rightarrow CH_3+H_2$ [14.93 kcal/mol (Ref. 68) and 10.84 kcal/mol (Ref. 69) for barrier height and threshold energy, respectively]. The small cross section of the latter reaction (generally less than 0.2 $Å^2$) has made state-to-state dynamics experiments difficult. Consequently, the $SiH_4+H\rightarrow SiH_3+H_2$ reaction may be a better candidate for detailed state-resolved experimental studies, however, as noted in Sec. I, the experimental dynamics work is still lacking.

B. H_2 rovibrational population and reaction mechanism

In order to gain some insights into the reaction mechanism, three batches of 25 000 trajectories were run at $E_{coll}=9.41$ kcal/mol for $b=0,1.2,1.9$ Å, respectively. Table I lists the H_2 vibrational populations calculated on the WSB surface for selected impact parameters. As can be seen, most H_2 molecules are in the ground vibrational state, and the population at $v'=1$ accounts for less than 20.0%. The corresponding H_2 $(v'=0)$ and H_2 $(v'=1)$ rotational distributions are depicted in Fig. 2.

As shown in Fig. 2(a), the rotational distribution for H_2 $(v'=0)$ peaks around $j'=1$ at $b=0.0$ Å, then $j'=2$ at $b=1.2$ Å, finally $j'=3$ at $b=1.9$ Å. Similar trend is also observed for H_2 $(v'=1)$ as seen from Fig. 2(b). It is clear that H_2 rotational distributions are strongly dependent on the impact parameter and higher rotationally excited H_2 could be promoted as impact parameter increases. This kind of rotational distribution shift suggests the existence of two competitive reaction mechanisms: rebound and stripping.

The rebound mechanism is well-known for this kind of H abstraction reaction, which is characteristic of a collinear $X-H'-H''$ $(X=C,Si,\ldots)$ transition-state configuration. For example, the $H+CD_4$ reaction has long been considered to proceed through a rebound mechanism in which the incident H atom is directed along a C–D bond and the HD product rebounds backward while the CD_3 fragment goes forward to conserve the linear momentum. However, the stripping mechanism has recently been proposed in a combined experimental and theoretical study on the reaction of H $+CD_4$,[70] in which the velocity of the H atom is perpendicular

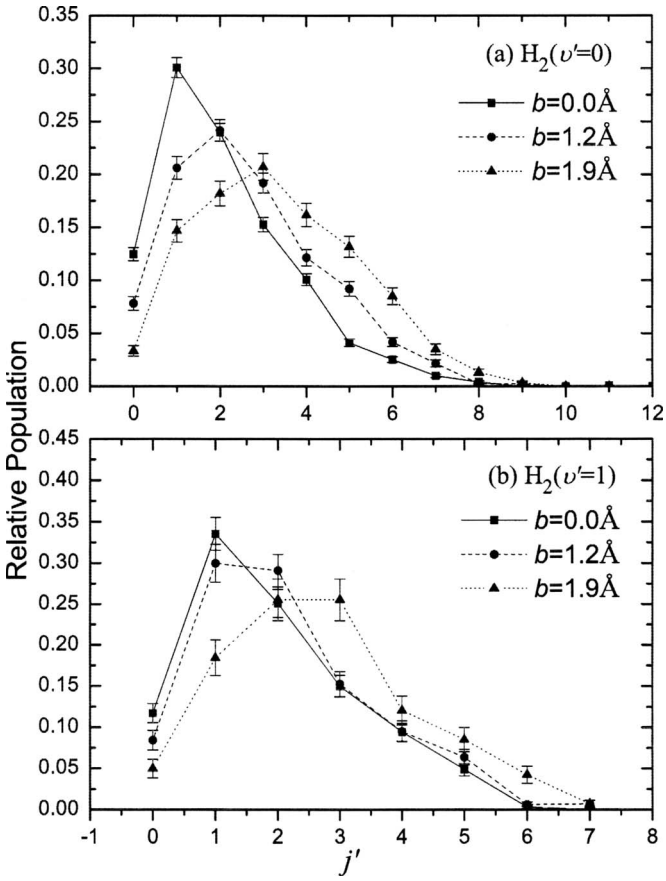

FIG. 2. Vibrationally state-resolved rotational distributions of H_2 at the collision energy of 9.41 kcal/mol for the impact parameters $b=0,1.2,1.9$ Å, respectively. The initial SiH_4 molecule is in its rovibrational ground state.

to the C–D bond and the HD product is carried into the forward hemisphere while the backward-scattered CD_3 is yielded. The stripping mechanism was further confirmed by Bowman *et al.*[67] in their QCT study on $CH_4+H\rightarrow CH_3+H_2$. It was pointed out by Bowman *et al.*[67] that the rebound mechanism is dominant for small impact parameters, while the stripping mechanism is favored at large impact parameters.

For the SiH_4+H reaction studied here, when the rebound mechanism dominates at small impact parameters, the incoming H atom collides with $H-SiH_3$ face to face along the central Si–H bond, yielding the H_2 product that rebounds in the backward direction with lower rotational energy. On the other hand, when the stripping mechanism dominates at large impact parameters, the incoming H atom attacks SiH_4 from the side face with an initial angle perpendicular to the Si–H bond. After such collision, the torque forward could make the H_2 product have higher rotational energy. So the above two mechanisms could be reflected by the rotational distribution shift with impact parameter shown in Fig. 2. The existence of these two mechanisms is also confirmed by direct observation of trajectories from our calculations. In this respect, $SiH_4+H\rightarrow SiH_3+H_2$ is similar to $CH_4+H\rightarrow CH_3+H_2$, and may be used as a second example of the newly observed stripping mechanism.

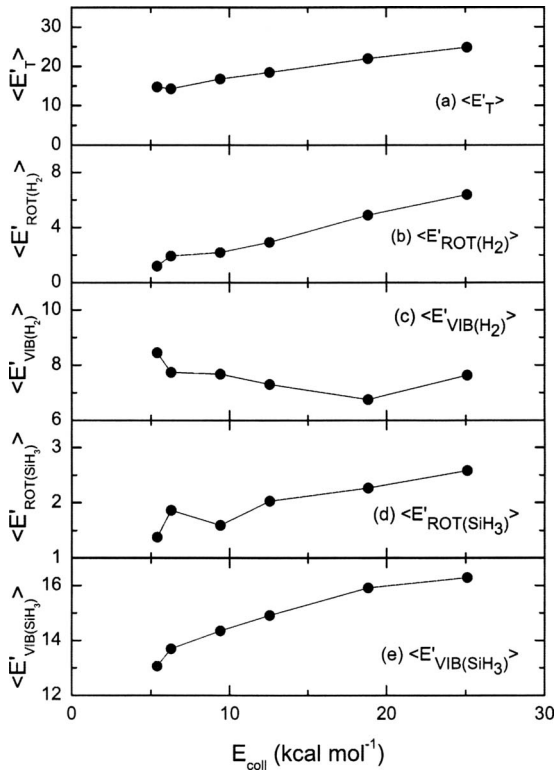

FIG. 3. Average energy (in kcal/mol) in products as a function of collision energy for the $SiH_4+H \rightarrow SiH_3+H_2$ reaction: (a) average product relative translational energy, (b) average H_2 rotational energy, (c) average H_2 vibrational energy, (d) average SiH_3 rotational energy, and (e) average SiH_3 vibrational energy. The initial SiH_4 molecule is in its rovibrational ground state, and the impact parameter is randomly chosen between 0 and b_{max}.

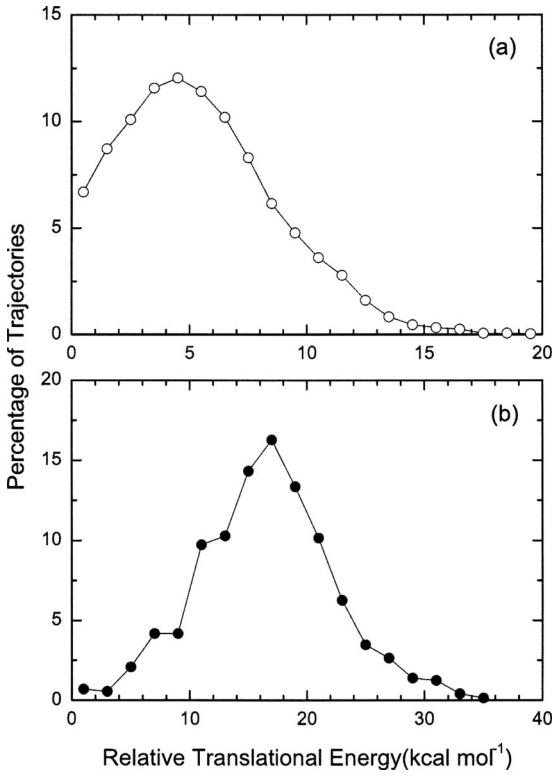

FIG. 4. Relative translational energy distributions for (a) nonreactive and (b) reactive collisions with the impact parameter set to zero. The results in (a) are obtained using a bin size of 1 kcal/mol, whereas the bin size for (b) is 2 kcal/mol.

C. Product energy distributions and collision energy transfer

Figure 3 displays the average product energies as a function of collision energy (b is randomly chosen between 0 and b_{max}). As can be seen, average product relative translational energy, average SiH_3 vibrational energy, and average H_2 rotational energy almost increase linearly with the collision energy. As for the product SiH_3, average vibrational energy [see Fig. 3(e)] increases from 13.7 to 16.3 kcal/mol with the increase in collision energy, which implies that the vibration of SiH_3 shifts from the ground state to the excited state since the vibrational energy for the ground state is 13.5 kcal/mol, whereas that for the first-excited state (have one quantum of excitation in the low-frequency umbrella-bending mode) is 15.7 kcal/mol. It seems that the SiH_3 umbrella vibrational mode is excited with the increase in collision energy. As for the other product H_2, the average vibrational energy [see Fig. 3(c)] is in the range of 6.7–8.4 kcal/mol for all reactive collisions at E_{coll}=5.40–25.10 kcal/mol, which indicates that a great number of H_2 molecules are in the ground vibrational state (the ground vibrational energy is 6.3 kcal/mol, and the first-excited vibrational energy is 18.9 kcal/mol). This is understandable since the large energy difference (12.6 kcal/mol) between the first-excited and ground states makes it difficult to reach the first-excited vibrational state of H_2.

Table II shows the average fraction of the relative translational energy in reactive products as a function of collision energy. Interestingly, the fraction of the relative translational energy with respect to the total available energy is roughly constant (about 40%) at all collision energies, and the remaining fraction of the total available energy (about 60%) is redistributed into the product vibrational and rotational degrees of freedom. Figure 4 shows the product relative translational energy distributions for both nonreactive and reactive collisions at b=0, which peak around 5 and 17 kcal/mol, respectively. The corresponding vibrational energy distributions are depicted in Fig. 5, which indicates that the peaks of SiH_4, SiH_3, and H_2 distributions appear in the region of vibrational ground state. As shown in Fig. 6, the

TABLE II. The average translational energy ($\langle E_T' \rangle$) of reactive products is given as a percentage of the total available energy (E_{av}) at different collision energies (E_{coll}), in which the initial SiH_4 is fixed in its rovibrational ground state (about 19.6 kcal/mol). All energies are in kcal/mol.

E_{coll} (kcal/mol)	5.40	6.28	9.41	12.55	18.83	25.10
$\langle E_T' \rangle$ (kcal/mol)	14.76	14.29	16.78	18.44	21.95	24.83
E_{av} (kcal/mol)	38.81	39.69	42.82	45.96	54.24	58.51
Percentage of $\langle E_T' \rangle$	38.04	36.00	39.18	40.13	42.02	42.44

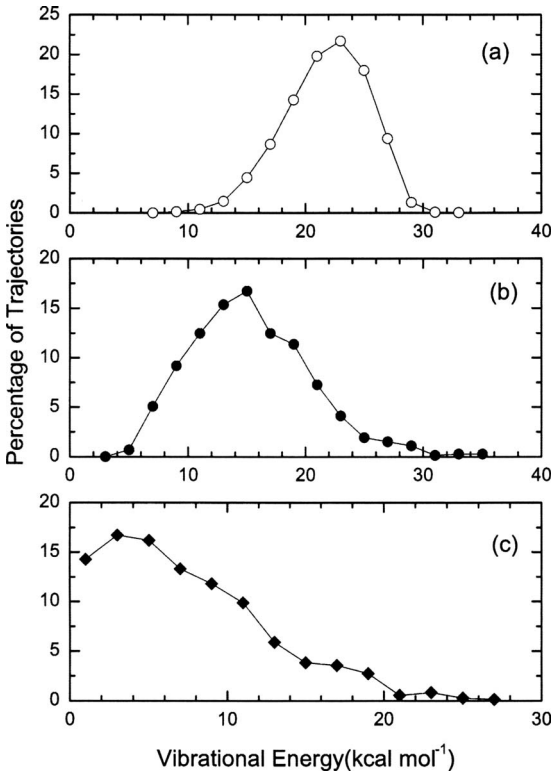

FIG. 5. Vibrational energy distributions of products: (a) SiH_4 for nonreactive collisions and (b) SiH_3 and (c) H_2 for reactive collisions. The initial SiH_4 molecule is in its rovibrational ground state and the impact parameter is set to zero. All the distributions are obtained using the bin size of 2 kcal/mol.

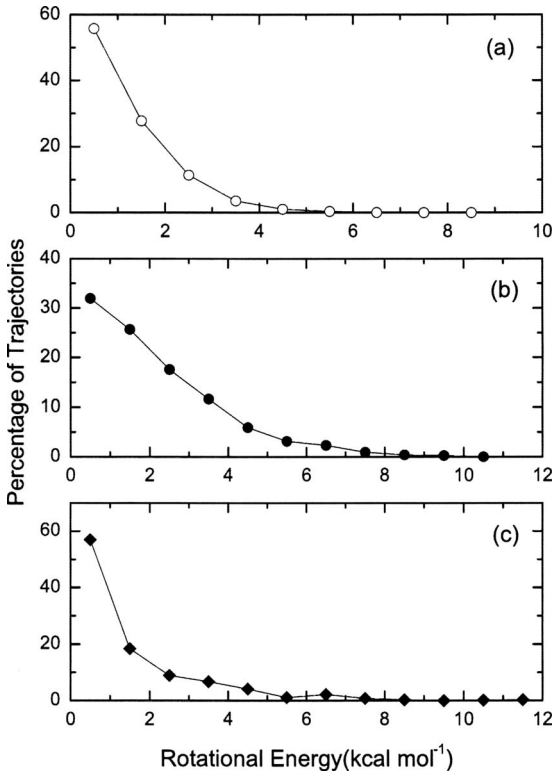

FIG. 6. Rotational energy distributions of products: (a) SiH_4 for nonreactive collisions and (b) SiH_3 and (c) H_2 for reactive collisions. The initial SiH_4 molecule is in its rovibrational ground state and the impact parameter is set to zero. All the distributions are obtained using the bin size of 1 kcal/mol.

rotational energy distributions of SiH_4, SiH_3, and H_2 indicate that the scattered fragments seldom appear with high rotational energy, and this results from the collinear rebound mechanism at $b=0$.

The average translational, rotational, and vibrational energies of products for the nonreactive and reactive SiH_4+H collisions are summarized in Table III. For nonreactive collisions, the total available energy includes the initial relative translational energy (9.41 kcal/mol) and the initial vibrational energy of SiH_4 (19.6 kcal/mol), while for reactive collisions, the 13.81 kcal/mol of energy difference between products and reactants should also be included. For nonreactive collisions, as shown in Table III, the average relative translational energy between SiH_4 and H fragments decreases by 3.96 kcal/mol after collision (from 9.41 to 5.45 kcal/mol). On the other hand, the average vibrational energy of SiH_4 increases by 2.74 kcal/mol (from 19.6 to 22.34 kcal/mol). whereas the SiH_4 rotational energy increases by 1.11 kcal/mol after collision. So, more than 40% of the initial relative translational energy is transferred into the vibrational and rotational energies of SiH_4 after nonreactive collisions. This differs from that observed in CH_4+H nonreactive collisions,[24] in which the relative translational energy changes little after collision. A possible explanation for this is that the bonds in SiH_4 are much weaker than those in CH_4.

As for reactive collisions, as displayed in Table III, the final average relative translational energy between SiH_3 and H_2 fragments increases to 16.51 kcal/mol. On the other hand, SiH_3 gains the average vibrational energy of 15.28 kcal/mol and rotational energy of 2.10 kcal/mol, whereas H_2 acquires the vibrational energy of 7.44 kcal/mol and rotational energy of 1.48 kcal/mol. Obviously, all the translational, vibrational, and rotational energies become larger after collision. This is understandable since the title reaction is exothermic by about 13.81 kcal/mol (57.78 kJ/mol), which may be redistributed into the product translational, vibrational, and rotational degrees of freedom.

D. Thermal rate coefficient

The thermal rate coefficient for the $SiH_4+H \rightarrow SiH_3+H_2$ reaction was calculated with the QCT method for the temperature range of 300–1600 K. Since most SiH_4 molecules are in the ground vibrational state at very low temperatures (e.g., more than 95% of SiH_4 molecules are in the ground vibrational state at 300 K), the initial vibrational state of SiH_4 was chosen as the ground state using the fixed normal mode sampling for calculations below 400 K. However, vibrationally excited SiH_4 molecules have a noticeable influence on the rate coefficient at higher temperatures (400–1600 K), and in these cases, the initial vibrational energy of SiH_4 molecule was thermally sampled.

Figure 7 shows Arrhenius plots of our calculated rate coefficients for the SiH_4+H reaction, together with the previous experimental and theoretical results. The dashed line with triangles and solid line with circles display those obtained from the present QCT and QCT-ZPE calculations on the WSB surface, respectively. For comparison, the rate co-

TABLE III. The total available energy (E_{av}) and the average translational ($\langle E'_T \rangle$), vibrational ($\langle E'_{vib} \rangle$), and rotational energies ($\langle E'_T \rangle$) of products for the nonreactive and reactive SiH_4+H collisions at $b=0$. The initial SiH_4 is fixed in its rovibrational ground state (about 19.6 kcal/mol), and the initial relative translational energy is set to 9.41 kcal/mol. All energies are in kcal/mol.

Nonreactive collision	E_{av} 29.01	$\langle E'_T \rangle$ 5.45	$\langle E'_{vib} \rangle(SiH_4)$ 22.34		$\langle E'_{rot} \rangle(SiH_4)$ 1.11	
Reactive collision	E_{av} 42.82	$\langle E'_T \rangle$ 16.51	$\langle E'_{vib} \rangle(SiH_3)$ 15.28	$\langle E'_{rot} \rangle(SiH_3)$ 2.10	$\langle E'_{vib} \rangle(H_2)$ 7.44	$\langle E'_{rot} \rangle(H_2)$ 1.48

efficients calculated with the improved canonical variational transition state theory plus the small-curvature tunneling correction (ICVT/SCT) method[22] on the same surface and several experimental results[10–13,15,16] are also placed in the figure. As can be seen from Fig. 7, the QCT-ZPE rate coefficients are in generally good agreement with the experimental results. From 290 to 660 K, the QCT-ZPE rate coefficients are in better agreement with the experimental results obtained by Goumri *et al.*[16] in 1993 and by Arthur and Miles[11] in 1997 than previous ICVT/SCT results. For instance, compared with the rate coefficient of 6.82×10^{-12} cm^3 $molecule^{-1}$ s^{-1} at 600 K by Goumri *et al.*,[16] the QCT-ZPE and previous ICVT/SCT results are $(5.20 \pm 0.77) \times 10^{-12}$ and 3.82×10^{-12} cm^3 $molecule^{-1}$ s^{-1}, respectively. At room temperature, the experimental rate coefficients by Koshi *et al.*[13] and by Loh and Jasinski[15] range from 4.0×10^{-13} to 2.0×10^{-13} cm^3 $molecule^{-1}$ s^{-1}, and the QCT-ZPE rate coefficient of $(2.72 \pm 1.22) \times 10^{-13}$ cm^3 $molecule^{-1}$ s^{-1} is within this range. However, it can be noticed from Fig. 7 that the QCT-ZPE rate coefficients at low temperatures show a weak non-Arrhenius behavior, which indicates that the ZPE leakage problem may not be completely solved; on the other hand, the tunneling effects are not taken into account in the present QCT calculations. Consequently, the very good agreement with experiment at low temperatures may be partly owing to a fortuitous cancellation of the ZPE leakage and the neglect of tunneling. Further quantum-mechanical calculations are required to find out as to what extent the tunneling effects may play a role. Furthermore, the difference between the QCT and QCT-ZPE results is very small at high temperatures (for example, the differences at 1600 and 1400 K account for 2.3% and 5.1% of the corresponding QCT rate coefficients, respectively), but a significant difference appears at low temperatures, which results from the ZPE problem in QCT calculations. Since at low temperatures, the relative translational energy between SiH_4 and H is relatively small, the ZPE constraint in the transition state becomes very important, leading to the noticeable difference between the results with and without the ZPE correction. It is encouraging to see that for the 12-dimensional reactive system studied in this work there is good agreement between the rate coefficients calculated with the ZPE-corrected QCT method and those measured experimentally.

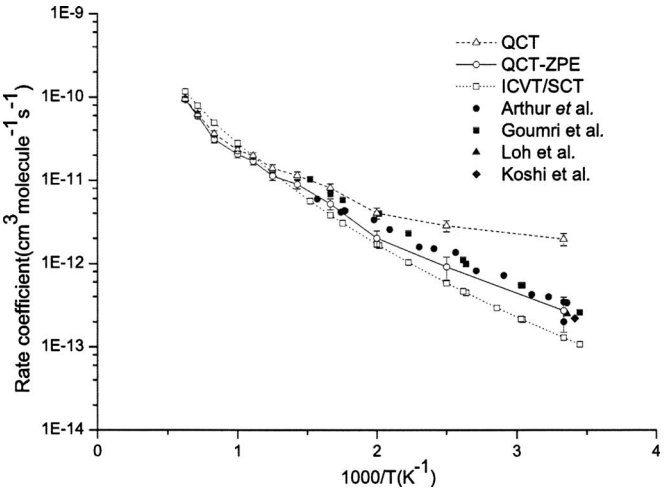

FIG. 7. The thermal rate coefficients for the $SiH_4+H \rightarrow SiH_3+H_2$ reaction are plotted as function of 1000/T. The dashed line with triangles and solid line with circles correspond to the present QCT and QCT-ZPE calculations on the WSB surface, while the dotted line with squares refers to the previous calculations (Ref. 22) with the ICVT/SCT method on the same surface; closed, circle, closed square, closed triangle, and close diamond are from experimental results of Refs. 10–12, 16, 15, and 13, respectively.

IV. SUMMARY

We performed detailed QCT studies on the recent global 12-dimensional *ab initio* interpolated PES for the $SiH_4+H \rightarrow SiH_3+H_2$ reaction. The excitation function was reported and the cross section was estimated to be more than eight times larger than that for the $CH_4+H \rightarrow CH_3+H_2$ reaction at the same collision energy. At the collision energy of 9.41 kcal/mol, product energy distributions and rovibrational populations were investigated in detail. The H_2 rotational populations display a strong dependence on the impact parameter, which indicates that the abstraction reaction mechanism is a combination of rebound and stripping. So the SiH_4+H reaction could serve as another example of the stripping mechanism, which was first observed in the $H+CD_4$ reaction in 2005. Furthermore, the thermal rate coefficient for the temperature range of 300–1600 K has been obtained, and the ZPE-corrected QCT rate coefficient shows good agreement with the available experimental data.

ACKNOWLEDGMENTS

This work is supported by National Natural Science Foundation of China (Nos. 20573119 and 20733005), and National Key Basic Research Project (973) of China (No. 2007CB815204). Most calculations of this research were performed at the Virtual Laboratory of Computational Chemistry, Computer Network Information Center, Chinese Academy of Sciences. The authors would like to thank Professor William L. Hase for his provision of VENUS96 program.

[1] H. Niki and G. J. Mains, J. Phys. Chem. **68**, 304 (1964).

[2] J. R. Doyle, D. A. Doughty, and A. Gallagher, J. Appl. Phys. **69**, 4169 (1991).
[3] M. J. Kushner, J. Appl. Phys. **63**, 2532 (1988).
[4] A. Talbot, J. Arcamone, C. Fellous, F. Deleglise, and D. Dutartre, Mater. Sci. Semicond. Process. **8**, 21 (2004).
[5] K. Obi, H. S. Sandhu, H. E. Gunning, and O. P. Strausz, J. Phys. Chem. **76**, 3911 (1972).
[6] J. A. Cowfer, K. P. Lynch, and J. V. Michael, J. Phys. Chem. **79**, 1139 (1975).
[7] K. Y. Choo, P. P. Gaspar, and A. P. Wolf, J. Phys. Chem. **79**, 1752 (1975).
[8] E. R. Austin and F. W. Lampe, J. Phys. Chem. **81**, 1134 (1977).
[9] D. Mihelcic, V. Schubert, R. N. Schindler, and P. Potzinger, J. Phys. Chem. **81**, 1543 (1977).
[10] N. L. Arthur, P. Potzinger, B. Reimann, and H. P. Steenbergen, J. Chem. Soc., Faraday Trans. 2 **85**, 1447 (1989).
[11] N. L. Arthur and L. A. Miles, J. Chem. Soc., Faraday Trans. **93**, 4259 (1997).
[12] N. L. Arthur and L. A. Miles, Chem. Phys. Lett. **282**, 192 (1998).
[13] M. Koshi, F. Tamura, and H. Matsui, Chem. Phys. Lett. **173**, 235 (1990).
[14] N. M. Johnson, J. Walker, and K. S. Stevens, J. Appl. Phys. **69**, 2631 (1991).
[15] S. K. Loh and J. M. Jasinski, J. Chem. Phys. **95**, 4914 (1991).
[16] A. Goumri, W.-J. Yuan, L. Ding, Y. Shi, and P. Marshall, Chem. Phys. **177**, 233 (1993).
[17] M. S. Gordon, D. R. Gano, and J. A. Boatz, J. Am. Chem. Soc. **105**, 5771 (1983).
[18] A. Tachibana, Y. Kurosaki, K. Yamaguchi, and T. Yamabe, J. Phys. Chem. **95**, 6849 (1991).
[19] K. D. Dobbs and D. A. Dixon, J. Phys. Chem. **98**, 5290 (1994).
[20] J. Espinosa-García, J. Sansón, and J. C. Corchado, J. Chem. Phys. **109**, 466 (1998).
[21] X. Yu, S. M. Li, Z. S. Li, and C. C. Sun, J. Phys. Chem. A **104**, 9207 (2000).
[22] M. Wang, X. Sun, W. Bian, and Z. Cai, J. Chem. Phys. **124**, 234311 (2006).
[23] W. Wang, S. Feng, and Y. Zhao, J. Chem. Phys. **126**, 114307 (2007).
[24] K. C. Thompson, M. J. T. Jordan, and M. A. Collins, J. Phys. Chem. **108**, 8302 (1998); M. A. Collins, Theor. Chem. Acc. **108**, 313 (2002); R. P. A. Bettens and M. A. Collins, J. Chem. Phys. **111**, 816 (1999); K. C. Thompson and M. A. Collins, J. Chem. Soc., Faraday Trans. **93**, 871 (1997).
[25] T. D. Sewell and D. L. Thompson, Int. J. Mod. Phys. B **11**, 1067 (1997).
[26] F. J. Aoiz, L. Bañares, and V. J. Herrero, J. Chem. Soc., Faraday Trans. **94**, 2483 (1998).
[27] F. J. Aoiz, L. Bañares, M. J. D'Mello, V. J. Herrero, V. S. Rábanos, L. Schnieder, and R. E. Wyatt, J. Chem. Phys. **101**, 5781 (1994).
[28] L. Schnieder, K. Seekamp-Rahn, J. Borkowski, E. Wrede, K. H. Welge, F. J. Aoiz, L. Bañares, and M. J. D'Mello, Science **269**, 207 (1995).
[29] D. M. Neumark, A. M. Wodtke, G. N. Robinson, C. C. Hayden, K. Shobatake, R. K. Sparks, T. P. Schafer, and Y. T. Lee, J. Chem. Phys. **82**, 3067 (1985).
[30] F. J. Aoiz, L. Bañares, V. J. Herrero, V. S. Rábanos, K. Stark, and H.-J. Werner, Chem. Phys. Lett. **223**, 215 (1994).
[31] F. J. Aoiz, L. Bañares, V. J. Herrero, V. S. Rábanos, K. Stark, and H.-J. Werner, J. Chem. Phys. **102**, 9248 (1995).
[32] M. Alagia, N. Balucani, L. Cartechini, P. Casavecchia, E. H. van Kleef, G. G. Volpi, F. J. Aoiz, L. Bañares, D. W. Schwenke, T. C. Allison, S. L. Mielke, and D. G. Truhlar, Science **273**, 1519 (1996).
[33] N. Balucani, L. Cartechini, P. Casavecchia, G. G. Volpi, F. J. Aoiz, L. Bañares, M. Menéndez, W. Bian, and H.-J. Werner, Chem. Phys. Lett. **328**, 500 (2000).
[34] F. J. Aoiz, L. Bañares, J. F. Castillo, D. Skouteris, and H.-J. Werner, J. Chem. Phys. **115**, 2074 (2001).
[35] C. Shen, T. Wu, G. Ju, and W. Bian, Chem. Phys. **272**, 61 (2001).
[36] G. C. Schatz, A. Papaioannou, L. A. Pederson, L. B. Harding, T. Hollebeek, T.-S. Ho, and H. Rabitz, J. Chem. Phys. **107**, 2340 (1997).
[37] A. J. Alexander, D. A. Blunt, M. Brouard, J. P. Simons, F. J. Aoiz, L. Bañares, Y. Fujimura, and M. Tsubouchi, Faraday Discuss. **108**, 375 (1997).
[38] J. F. Castillo and J. Santamaría, J. Phys. Chem. A **104**, 10414 (2000).
[39] J. F. Castillo, F. J. Aoiz, L. Bañares, and J. Santamaría, Chem. Phys. Lett. **329**, 517 (2000).
[40] J. F. Castillo, F. J. Aoiz, and L. Bañares, Chem. Phys. Lett. **356**, 120 (2002).
[41] J. F. Castillo, M. A. Collins, F. J. Aoiz, and L. Bañares, J. Chem. Phys. **118**, 7303 (2003).
[42] J. F. Castillo, F. J. Aoiz, L. Bañares, and M. A. Collins, J. Phys. Chem. A **108**, 6611 (2004).
[43] E. P. Wallis and D. L. Thompson, J. Chem. Phys. **97**, 4929 (1992).
[44] A. J. C. Varandas and L. Zhang, Chem. Phys. Lett. **402**, 399 (2005).
[45] D. Troya and E. García-Molina, J. Phys. Chem. A **109**, 3015 (2005).
[46] D. Troya, J. Phys. Chem. A **109**, 5814 (2005).
[47] J. F. Castillo, F. J. Aoiz, L. Bañares, E. Martinez-Nuñez, A. Fernández-Ramos, and S. Vazquez, J. Phys. Chem. A **109**, 8459 (2005).
[48] E. García, C. Sánchez, A. Saracibar, and A. Laganà, J. Phys. Chem. A **108**, 8752 (2004).
[49] C. Rangel, J. Espinosa-García, and J. C. Corchado, J. Phys. Chem. A **109**, 8071 (2005).
[50] M. Karplus, R. N. Porter, and R. D. Sharma, J. Chem. Phys. **43**, 3259 (1965).
[51] R. N. Porter and L. M. Raff, in *Dynamics of Molecular Collision, Part B*, edited by W. H. Miller (Plenum, New York, 1976), p. 1.
[52] R. N. Porter, Annu. Rev. Phys. Chem. **25**, 317 (1974).
[53] L. M. Raff and D. L. Thompson, in *Theory of Chemical Reaction Dynamics*, edited by M. Baer (CRC, Boca Raton, FL, 1985), Vol. III, p. l.
[54] H. R. Mayne, in *Dynamics of Molecules and Chemical Reactions*, edited by R. E. Wyatt and J. Z. H. Zhang (Dekker, New York, 1996), p. 589.
[55] G. H. Peslherbe, H. Wang, and W. L. Hase, Adv. Chem. Phys. **105**, 171 (1999).
[56] W. L. Hase, R. J. Duchovic, X. Hu *et al.*, Quantum Chemistry Program Exchange (QCPE) Bulletin **16**, 671 (1996).
[57] E. B. Wilson, Jr., J. C. Decius, and P. C. Cross, *Molecular Vibrations* (McGraw-Hill, New York, 1955), p. 285.
[58] M. C. Gutzwiller, *Chaos in Classical and Quantum Mechanics* (Springer, New York, 1990).
[59] W. Press, S. Teukolsky, W. Vetterling, and B. Flannery, *Numerical Recipies in C. The Art of Scientific Computing*, 2nd ed. (Cambridge University Press, Cambridge, 1992).
[60] X. Wang, M. Ben-Nun, and R. D. Levine, Chem. Phys. **197**, 1 (1995).
[61] J. M. C. Marques, E. Martínez-Nüñez, A. Fernández-Ramos, and S. A. Vázquez, J. Phys. Chem. A **109**, 5415 (2005).
[62] T. D. Sewell, D. L. Thompson, J. D. Gezelter, and W. H. Miller, Chem. Phys. Lett. **193**, 512 (1992).
[63] Y. Guo, D. L. Thompson, and T. D. Sewell, J. Chem. Phys. **104**, 576 (1996).
[64] S.-F. Wu and R. A. Marcus, J. Chem. Phys. **53**, 4026 (1970); J. M. Bowman and A. Kuppermann, *ibid.* **59**, 6524 (1973); D. G. Truhlar, J. Phys. Chem. **83**, 188 (1979); G. C. Schatz, J. Chem. Phys. **79**, 5386 (1983); D. Lu and W. L. Hase, *ibid.* **89**, 6723 (1988); G. Stock and U. Müller, *ibid.* **111**, 65 (1999).
[65] A. J. C. Varandas, Chem. Phys. Lett. **225**, 18 (1994).
[66] A. J. C. Varandas, J. Chem. Phys. **99**, 1076 (1993).
[67] Z. Xie, J. M. Bowman, and X. Zhang, J. Chem. Phys. **125**, 133120 (2006).
[68] T. Wu, H.-J. Werner, and U. Manthe, J. Chem. Phys. **124**, 164307 (2006).
[69] A. J. C. Varandas, P. J. S. B. Caridade, J. Z. H. Zhang, Q. Cui, and K. Han, J. Chem. Phys. **125**, 064312 (2006).
[70] J. P. Camden, H. A. Bechtel, D. J. A. Brown, M. R. Martin, R. N. Zare, W. Hu, G. Lendvay, D. Troya, and G. C. Schatz, J. Am. Chem. Soc. **127**, 11898 (2005); J. P. Camden, W. F. Hu, H. A. Bechtel, D. J. A. Brown, M. R. Martin, R. N. Zare, G. Lendvay, D. Troya, and G. C. Schatz, J. Phys. Chem. A **110**, 677 (2006); W. Hu, G. Lendvay, D. Troya, G. C. Schatz, J. P. Camden, H. A. Bechtel, D. J. A. Brown, M. R. Martin, and R. N. Zare, *ibid.* **110**, 3017 (2006).